Temperature dependence of the lower critical field and strong pinning in high-temperature superconductors

Dragomir Davidović and Ljiljana Dobrosavljević-Grujić
Institute of Physics, P.O. Box 57, 11001 Belgrade, Yugoslavia
(Received 27 September 1990)

We show, within the framework of the Ginzburg-Landau theory, that both the conventional and the anomalous temperature dependence of the lower critical field observed in high-temperature superconductors may result from the flux penetration through a set of separated microdefects. Microdefects modeled by normal layers with proximity-induced superconductivity can produce drastic enhancement of the lower critical field at low temperatures and can provide strong-pinning centers. The pinning interaction between an isolated vortex and the normal layer is primarily magnetic at high temperatures. At low temperatures, magnetic interaction is reduced, due to the increase of the normal-layer coherence length.

I. INTRODUCTION

One of the intriguing features of high-T_c (HTC) superconducting single crystals is the temperature dependence of the lower critical field $H_{c1}(T)$. There are two qualitatively different types of the experimental results. One is the conventional BCS-like behavior exhibiting linear temperature dependence near T_c and negative curvature at lower temperatures, observed both in dc and ac magnetization measurements.[1,2] In the other, anomalous temperature dependence there are two regimes: from T_c down to approximately $0.5T_c$ $H_{c1}(T)$ is linear or with small positive curvature; at lower temperatures $H_{c1}(T)$ rapidly increases giving positive curvature. This type of behavior was obtained by dc magnetization measurements.[3,4]

There have been several attempts to account for this anomalous $H_{c1}(T)$.[5-7] Hirashima and Matsuura[5] suggested that it comes from the change of the symmetry of the order parameter at a low T. Ye *et al.*[6] proposed a theory based on the assumption of anisotropic Cooper pairing. Koyama *et al.*[7] suggested that the anomalous $H_{c1}(T)$ comes from the intrinsic property of a flux line in a multilayer structure of the oxides superconductors. In this paper we claim that the source of the anomalous behavior of $H_{c1}(T)$ is intrinsic intragranular defects—normal phases, present even in high-quality single crystals.[8] In Y-Ba-Cu-O one possible origin[9] is the decomposition of the off-stoichiometric phase into an orthorhombic O_7 structure and a tetragonal O_6 structure, preceded by a series of transient oxygen-ordered structures. Recent electron microscopy evidence[10] shows that typical dimensions of defects in Y-Ba-Cu-O vary from 20 to 1000 Å. When such microdefects are near specimen boundaries, H_{c1} can be lowered due to the flux penetration, in the form of quantized vortices[11] through the normal "channels." We model these defects by superconductor–normal-metal–superconductor (SNS) junctions. Coherence through the normal (N) regions is established by proximity effect. Common features of HTC superconductors are that at $T = 0$ the coherence length ξ_c along the c direction (perpendicular to CuO_2 layers) is very small and comparable to the lattice constant, and that the Ginzburg-Landau (GL) parameter κ is much greater than 1. In N defects, the coherence length $\xi_N(T)$ is temperature dependent, but its characteristic value $\xi_N(T_c)$ is presumably comparable to ξ_c, since the structure of the superconducting (S) phase and of the microdefects, which are easily formed parallel to CuO_2 layers, is similar. Starting from a *single* normal defect in single crystal, we show that the thickness of this defect, which provides anomalous $H_{c1}(T)$ dependence, is significantly greater than $\xi_N(T_c)$ and extends over the region of several unit cells. Therefore, anomalous $H_{c1}(T)$ dependence is not an intrinsic property of the superconducting phase.

In Sec. II we study the flux penetration and the pinning of an isolated vortex in a SNS junction. The material parameters will be chosen to correspond, first, to a typical conventional (artificial) SNS junction,[11] with large coherence length in N, and, second, to the SNS modeled defect, characterized by small coherence length in N.

In Sec. III we find $H_{c1}(T)$ in the limit $\kappa_S \gg 1$, $\xi_N \sim \xi_S$, and $a_N \ll \lambda_S$, where κ_S, ξ_S, and λ_S are the GL parameter, coherence length, and the penetration depth in S, respectively, and $2a_N$ is the N-layer thickness. This limit is crucial in understanding N defects in HTC oxides. The interaction between an isolated vortex and such defects suggests a strong pinning mechanism that would provide high critical current. A simple method, generalizing the conventional image method,[12] useful in theoretical treatment of such junctions, is given. Finally, an experiment that might prove this pinning mechanism, is suggested.

II. FLUX PENETRATION AND PINNING IN THE *SNS* JUNCTION

A. The entrance of the magnetic flux in the *SNS* junction

Consider the N layer of thickness $2a_N$ in the Y-Z plane, embedded in the S matrix. The magnetic field $\mathbf{H}$ is assumed parallel to z axis (Fig. 1). We begin by writing GL equations[13] for the order parameter ψ and the magnetic field $\mathbf{H} = \nabla \times \mathbf{A}$ in both N and S metals:

$$\alpha\psi + \beta|\psi|^2\psi + \frac{1}{2m^*}\left(\frac{\hbar}{i}\nabla - \frac{e^*}{c}\mathbf{A}\right)^2\psi = 0 , \tag{1}$$

$$\mathbf{j} = \frac{c}{4\pi}\nabla \times \mathbf{H} = \frac{e^*\hbar}{2m^*i}(\psi^*\nabla\psi - \psi\nabla\psi^*) - \frac{(e^*)^2}{m^*c}|\psi|^2\mathbf{A} . \tag{2}$$

Parameters α and β are piecewise constant functions of position taking on values $\alpha = \alpha_S = \alpha_S^0(T - T_{cS}) < 0$ and $\beta = \beta_S > 0$ in S and $\alpha = \alpha_N = \alpha_N^0(T - T_{cN}) > 0$ and $\beta = \beta_N > 0$ in N. T_{cS} and T_{cN} are the bulk critical temperatures of S and N, respectively. The critical temperature of the junction is $T_c = T_{cS}$. In general, the nonlinear term of the first GL equation is small in N and can be neglected; it does not qualitatively change the results when the temperature T is greater than the critical temperature T_{cN} of N.[14] The free-energy density is

$$F_1[\mathbf{r}, \mathbf{H}(\mathbf{r})] = \alpha|\psi|^2 + \frac{1}{2}\beta|\psi|^4 + \frac{\hbar^2}{2m^*}(\nabla|\psi|)^2 + \frac{m^*}{2}\left(\frac{c\nabla \times \mathbf{H}}{4\pi e^*|\psi|}\right)^2 + \frac{1}{8\pi}H^2 . \tag{3}$$

The coherence lengths $\xi_{S,N}$ and the GL parameters $\kappa_{S,N}$ for S and N are

$$\xi_{S,N}^2 = \frac{\hbar^2}{2m^*|\alpha_{S,N}|}, \quad \kappa_{S,N}^2 = \frac{1}{2\pi}\left(\frac{m^*c}{e^*\hbar}\right)^2\beta_{S,N} , \tag{4}$$

and the penetration depth in bulk superconductor λ_S is

$$\lambda_S^2 = \frac{m^*c^2}{4\pi(e^*)^2\psi_\infty^2} , \tag{5}$$

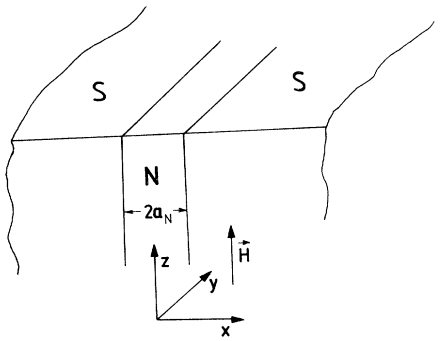

FIG. 1. Geometry for the calculation of the lower critical field H_{c1} and the force f acting on the vortex displaced in the x direction. Magnetic field $\mathbf{H}$ and the vortex are parallel to the normal (N) layer, embedded in the superconductor (S).

where $\psi_\infty^2 = -\alpha_S/\beta$ is the bulk square order parameter in zero field. At low fields the SNS junction exhibits a Meissner state, due to the proximity effect from the superconductors. If the field becomes larger than H_{c1} this state is destroyed and the magnetic field enters the junction. Flux may enter in the form of linear array of quantized vortices[11,15] or in the form of a plane parallel to N (laminar model). In a bulk superconductor, a vortex state is more favorable than the laminar state.[16] We shall examine whether this is valid in a SNS junction.

First, we assume the vortex model for the flux penetration. The critical field H_{c1} for the entrance of the first vortex is given by the difference between the free energies (per unit length) of the one-vortex and no-vortex states:

$$H_{c1} = \frac{4\pi}{\Phi_0}\int d^2\mathbf{r}\,\{F_1[\mathbf{r}, \mathbf{H}(\mathbf{r})] - F_0(\mathbf{r})\} . \tag{6}$$

We shall assume the variational form for the order parameter:[15]

$$\psi = \psi_\infty f(r)g(x)e^{i\phi} , \tag{7}$$

where $\phi = \tan^{-1}(y/x)$ and $g(x)$ is the zero-field solution of Eq. (1):

$$g(x) = \begin{cases} \tanh\left(\dfrac{b}{\sqrt{2}\xi_S}\right)\dfrac{\cosh[(x-c)/\xi_N]}{\cosh(a_N/\xi_N)}, & |x-c| < a_N \\ \tanh\left(\dfrac{|x-c|+b-a_N}{\sqrt{2}\xi_S}\right), & |x-c| \geq a_N , \end{cases} \tag{8}$$

the origin $x = 0$ being at the vortex position. Parameter b is chosen so that dg/dx is continuous at the SN boundary

$$b = \frac{\xi_S}{\sqrt{2}}\sinh^{-1}\left[\sqrt{2}\frac{\xi_N}{\xi_S}\coth\left(\frac{a_N}{\xi_N}\right)\right] .$$

Distance c between the vortex and the center of N is equal to zero in the calculation of H_{c1}. Function $f(r)$, introduced by Clem,[17]

$$f(r) = r/\sqrt{r^2 + \xi_v^2} , \tag{9}$$

describes the core of the vortex. Parameter ξ_v gives the vortex core radius. For simplicity, the anisotropy of the vortex core is neglected. Introducing reduced variables, $\rho = \mathbf{r}/\lambda_S$ and $h(\rho) = H(\mathbf{r})/\sqrt{2}H_c$, where $H_c = \Phi_0/2\pi\sqrt{2}\lambda_S\xi_S$, $a_N \to \lambda_S a_N$, $\xi \to \lambda_S\xi$, Eq. (6) becomes[15]

$$h_{c1} = \frac{\kappa_S}{4\pi}\int d^2\rho\Bigg\{ h^2 + \frac{2}{(fg)^2}\left[\left(\frac{\partial h}{\partial x}\right)^2 + \left(\frac{\partial h}{\partial y}\right)^2\right] + \left[\mathrm{sgn}(\alpha)\left(\frac{\xi_S}{\xi}\right)^2 g^2 + \frac{1}{\kappa_S^2}\left(\frac{dg}{dx}\right)^2 + \frac{1}{2}\left(\frac{\kappa}{\kappa_S}\right)^2 g^4\left(f^2+1\right)\right](f^2-1) + \frac{1}{\kappa_S^2} g\frac{\partial f}{\partial \rho}\left(g\frac{\partial f}{\partial \rho} + 2\frac{x}{\rho} f\frac{dg}{dx}\right)\Bigg\}, \tag{10}$$

where $h(\rho)$ is the solution of the equation

$$h - \frac{\partial}{\partial x}\frac{1}{(fg)^2}\frac{\partial h}{\partial x} - \frac{\partial}{\partial y}\frac{1}{(fg)^2}\frac{\partial h}{\partial y} = \frac{2\pi}{\kappa_S}\delta(x)\delta(y)\,, \tag{11}$$

and α, κ, and ξ refer to local values. In physical units line energy E is related to H_{c1} as $E = \Phi_0 H_{c1}/4\pi$ and in reduced units $\tilde{\varepsilon}=h_{c1}4\pi/\kappa_S$. For simplicity we introduce $\kappa_S/(4\pi)\tilde{\varepsilon} = \varepsilon = h_{c1}$. Using the limiting form[15] of the solution $h(\rho)$ when $\rho \to 0$

$$h(\rho) \equiv h(x,y) = h(0,0) - g^2(0)\rho^2/2\kappa_S\xi_v^2\,,$$

Eq. (10) can be transformed into

$$\varepsilon = \frac{h(0,0)}{2} + \frac{\kappa_S}{4}\int_{-\pi/2}^{\pi/2} du\left[g^4\xi_v^2\left(\frac{X_0(x)}{\cos u} + \frac{X_1(x)\cos u}{4}\right) + \frac{3g^2}{8\kappa_S^2}\cos^3 u\right], \tag{12}$$

where $x = \xi_v \tan u$, $X_0(x) = 0$ for $|x-c| > a_N$, $X_0(x) = -(\kappa_N/\kappa_S)^2$ for $|x-c| < a_N$, $X_1(x) = 1$ for $|x-c| > a_N$, and $X_1(x) = (\kappa_N/\kappa_S)^2$ for $|x-c| < a_N$. Line energy ε has to be minimized with respect to ξ_v. Magnetic energy $h(0,0)/2$ comes from the magnetic field and the supercurrents. Remaining part of ε is the core energy of the vortex.

Since Eq. (11) describes variation of the magnetic field at distance of the order 1, the choice of parameters $a_N \sim \xi_N \sim \xi_S = 1/\kappa_S \ll 1$ best modeling the microdefects in HTC superconductors would be inconvenient for a numerical treatment of Eq. (11). Therefore, we choose $\kappa_S = 5$, although in HTC superconductors $\kappa_S \gg 1$. To describe the classical SNS junction we put $\xi_N = 2$. For the SNS junction describing microdefects in HTC superconductors we take $\xi_N = 0.4$.

Introduction of the local penetration depth[11,15]

$$\lambda(x) = \lambda_S/g(x)$$

enables us to define the parameter κ_{SN} (Ref. 14) at the SN interface:

$$\kappa_{SN} = \lambda_B/\xi_N\,, \tag{13}$$

where $\lambda_B = \lambda(c + a_N)$. For a typical value $a_N/\xi_N=1$ we get $\kappa_{SN} = 0.47$ for $\xi_N = 2$ and $\kappa_{SN} = 1.9$ for $\xi_N = 0.4$. Small κ_{SN} characterizes conventional artificial SNS junctions in which the screening in the N layer is important[14] and the vortex is primarily located in N. When $\kappa_{SN} = 1.9$, screening in N is weak[14] and the field of the vortex penetrates deeper in S. The vortex field and supercurrent distribution are obtained solving Eq. (11) numerically. As an example, consider the supercurrent distribution around the vortex centered in the N layer with $\xi_N = 0.4$ represented in Fig. 2(a). The streamlines of the supercurrent, which also represent contours of constant magnetic field, show that the changes of the field in the direction perpendicular to the N layer (outside the core of the vortex) are small throughout N, except at the distance of the order of ξ_N from the SN boundary, which is smaller than λ_S. In the superconductor, field variations in this direction are stronger, resembling the common exponential decay of the external field near the surface. In the limit $a_N \ll 1$, $\kappa_S \gg 1$ and $\xi_N \sim \xi_S = 1/\kappa_S$, for the thickness $2a_N$ containing several coherence lengths ξ_N, the pattern in Fig. 2(a) would change into the supercurrent distribution around a vortex in the insulating barrier, having streamlines in N perpendicular to the interface. In this limit, the component of the supercurrent parallel to N acquires a jump across the barrier, which can be calculated analytically (see Sec. III).

To solve Eq. (11) for the vortex field, we have used the relaxation method, which is described in Ref. 15. This method is unreliable for thick N metal, and we apply it in the interval $a_N/\xi_N < 2.5$.

Next possibility is that the flux enters according to the laminar model. In this case the magnetic field has its maximum at the center of N ($x = 0$), where it destroys the proximity-induced superconductivity. We shall as-

sume the variational form for the order parameter,

$$\psi = \psi_\infty g(x) f_l(x) , \tag{14}$$

where $f_l(x) = \tanh(x/\xi_l)$ describes the region of destroyed superconductivity. For the external field $H^{\rm ext}$ parallel to N, Gibbs energy per junction unit height is

$$G_l = \Delta F - \frac{1}{4\pi} H^{\rm ext} \int d^2\mathbf{r}\, H(x) ,$$

where ΔF is the free-energy difference between the laminar and Meissner state and $H(x)$ is the local magnetic field. Then, introducing reduced units, we get the reduced Gibbs energy per unit area [$g_l = G_l/(\Phi_0/4\pi)(\sqrt{2}H_C)L_y$, L_y being the length of the SNS in the y direction]:

$$g_l = \frac{\kappa_S}{2\pi}\int_0^\infty dx \left\{ h^2 + \frac{1}{(f_l g)^2}\left(\frac{dh}{dx}\right)^2 + (f_l^2 - 1) \times \left[\frac{1}{2}\left(\frac{\kappa}{\kappa_S}\right)^2 g^4 (f_l^2+1) - I(x) g^4\right] + \frac{1}{\kappa_S^2} g^2 \left(\frac{df}{dx}\right)^2 \right\} - \frac{\kappa_S}{2\pi} 2h^{\rm ext} |a(0^+)| , \tag{15}$$

where $I(x) = 1$ for $|x-c| > a_N$, $I(x) = 0$ for $|x-c| < a_N$, and $|a(0^+)|$ is the reduced vector potential in the limit $x \to 0^+$ and in the gauge where ψ is real. It is obtained from the equation

$$d^2a/dx^2 = (f_l g)^2 a , \tag{16}$$

with the boundary conditions

$$\left(\frac{da}{dx}\right)_{x=0} = h(0) , \quad a(\infty) = 0 .$$

Equation (16) is obtained by taking the curl of the second GL equation, Eq. (2). Parameters $h(0)$ and ξ_l are obtained by minimizing g_l for fixed external field. Then, $h(0) = h^{\rm ext}$ and $\xi_l \approx 0.3$ for $\xi_N = 0.4$ and ξ_l increases from ≈ 0.3 to ≈ 1.6 when a_N/ξ_N increases from 0 to 2.5 for $\xi_N = 2$. In this way we get

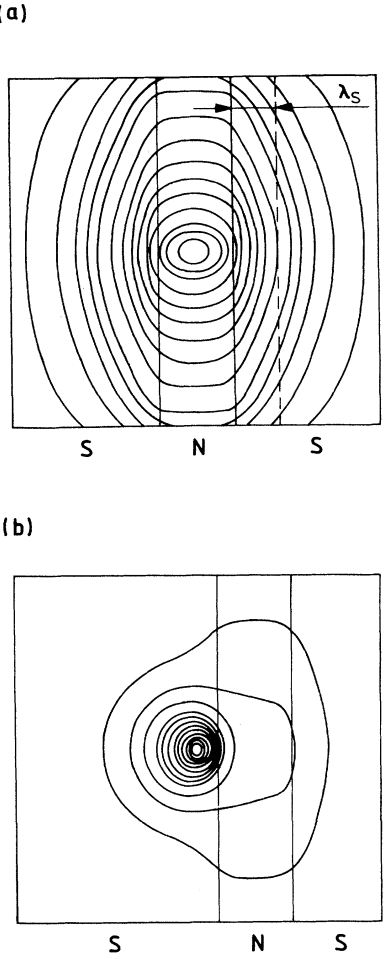

FIG. 2. (a) Supercurrent distribution around a single vortex in the middle of the normal layer N of thickness $2a_N = 1.6\lambda_s$. The coherence length and the GL parameter of N are $\xi_N = 0.4\lambda_S$ and $\kappa_N = 0.2$, respectively. The penetration depth λ_S gives the length scale over which the magnetic field enters the superconductors. The streamlines of the supercurrent, which seem perpendicular to the SN interface, show that the screening of the magnetic field is weak in N. (b) Supercurrent distribution produced by a vortex located in the superconductor at distance $0.4\lambda_S$ from the SN interface, for the same parameters as in (a).

$$g_l = \frac{\kappa_S}{2\pi}\int_0^\infty dx \left\{ (f_l^2-1) g^4 \left[\frac{1}{2}\left(\frac{\kappa}{\kappa_S}\right)^2 (f_l^2+1) - I(x)\right] + \frac{g^2}{\kappa_S^2}\left(\frac{df}{dx}\right)^2 \right\} - \frac{\kappa_S}{2\pi} h^{\rm ext} |a(0^+)| . \tag{17}$$

In obtaining Eq. (17) we used

$$\lim_{x\to+0} \frac{h(x)}{(f_l g)^2}\left(\frac{dh}{dx}\right) = h(0) a(0^+) .$$

The external field for the first flux entrance in the junction is obtained from $g_l = 0$. We find the critical field for the laminar entrance of the magnetic flux in N, for the same parameters as in the vortex model.

The results of the calculation are shown in Fig. 3 for $\xi_N = 2$ and in Fig. 4 for $\xi_N = 0.4$. The dependence of h_{c1} on a_N/ξ_N is exponential, except when a_N/ξ_N becomes small. The decay constant γ, defined by

$$h_{C1}(a_N/\xi_N) = h_{C1}(0) \exp\left(-\gamma \frac{a_N}{\xi_N}\right)$$

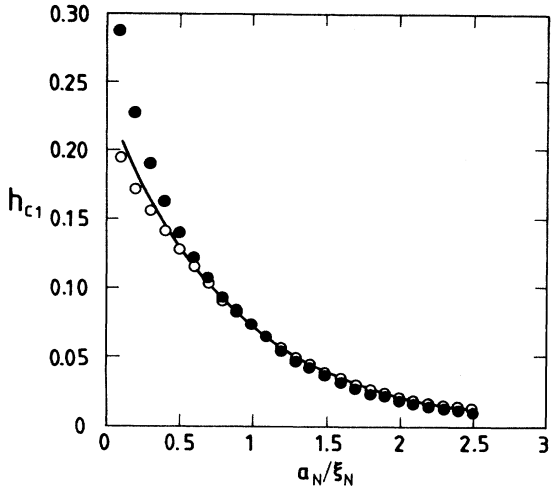

FIG. 3. Reduced critical field vs a_N/ξ_N for $\kappa_S = 5$, $\kappa_N = 0.2$, and $\xi_N = 2$: •, laminar solution; o, vortex solution. The solid curve is the best exponential fit to the vortex solution: $h_{c1} = 0.233\exp(-1.197 a_N/\xi_N)$.

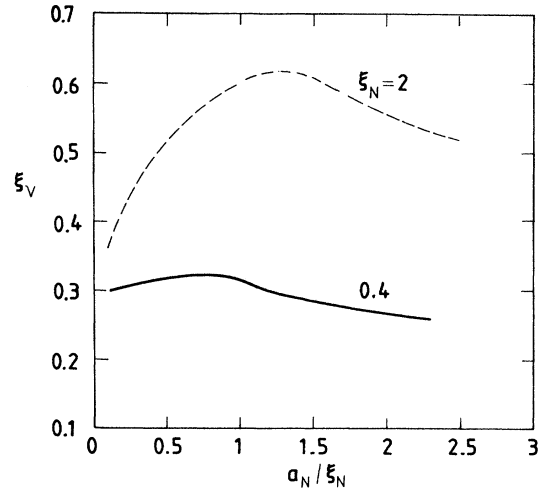

FIG. 5. Reduced variational parameter ξ_v vs a_N/ξ_N. Dashed line, $\xi_N = 2$; solid line, $\xi_N = 0.4$.

is equal to 1.2 for $\xi_N = 2$ and 0.9 for $\xi_N = 0.4$, for the vortex solution. For $\xi_N = 0.4$ magnetic flux enters in the form of vortices at any a_N/ξ_N, except near $a_N/\xi_N = 2.5$, when the two fields become approximately equal. For $\xi_N = 2$, the laminar solution gives h_{c1}, which is approximately equal to or even lower than h_{c1} determined from the vortex solution, when $a_N/\xi_N \approx 1$. We may conclude that flux enters in the form of an array of vortices in a larger interval of a_N/ξ_N for $\kappa_{SN} > 1$ than for $\kappa_{SN} < 1$. Expressing a_N in physical units, we obtain that the thickness when two fields become similar is $a_N \approx \lambda_S$ for $\xi_N = 0.4$ and $a_N \approx 2\lambda_S$ for $\xi_N = 2$, so that one may think that for $\kappa_{SN} < 1$ the SNS behaves as a "good" superconductor, allowing vortices for large N-metal thicknesses. In the SNS-modeled microdefects, when $a_N \ll \lambda_S$ and $\xi_N \sim \xi_S$, we may expect vortices in a very wide interval of a_N/ξ_N.

In Fig. 5 the dependence of the parameter ξ_v on a_N/ξ_N is plotted. For $\xi_N = 0.4$, ξ_v is weakly dependent on a_N/ξ_N, while for $\xi_N = 2$, ξ_v varies strongly showing maximum at $a_N/\xi_N \approx 1.5$.

B. Interaction between a single vortex and the normal layer

Let us suppose that the vortex changes the position relative to the N layer. The distance c in Eq. (8) becomes different from zero and ε in Eq. (12) is c dependent. Minimizing ε with respect to ξ_v, for fixed c, we obtain the position-dependent vortex line energy $\varepsilon(c)$, which is shown in Fig. 6. Line energy has a well-defined minimum

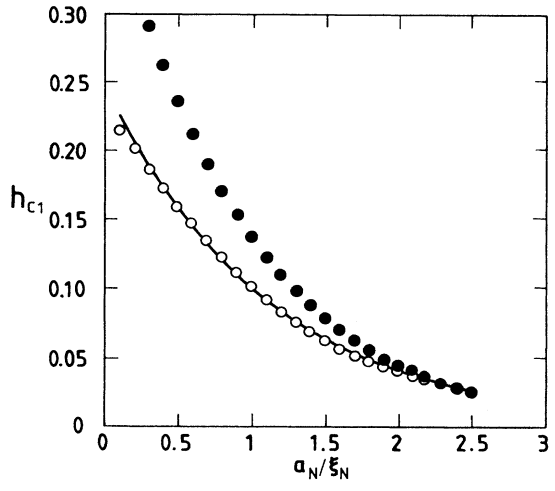

FIG. 4. Reduced lower critical field vs a_N/ξ_N for $\kappa_S = 5$, $\kappa_N = 0.2$, and $\xi_N = 0.4$: •, laminar solution; o, vortex solution. The solid curve is the best exponential fit to the vortex solution: $h_{c1} = 0.247\exp(-0.901 a_N/\xi_N)$.

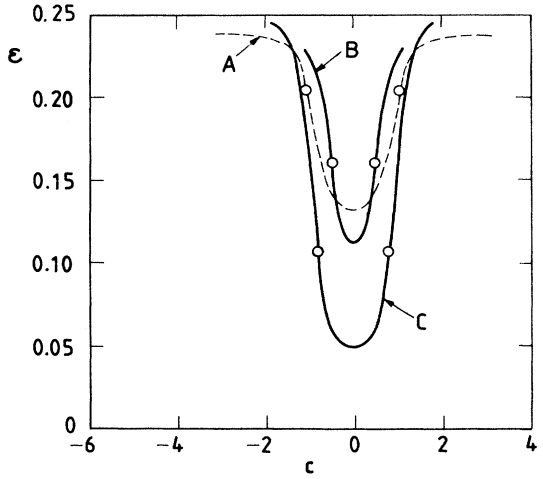

FIG. 6. Line energy ε vs vortex position c for $\kappa_S = 5$ and $\kappa_N = 0.2$: A, $\xi_N = 2$, $a_N/\xi_N = 0.5$ (dashed line); B, $\xi_N = 0.4$, $a_N/\xi_N = 1$ and C, $\xi_N = 0.4$, $a_N/\xi_N = 2$ (solid lines). The circles give the position of SN interfaces for each line. All quantities are in reduced units.

at the center of N, and it reaches the bulk value when $c \to \infty$. The force acting on the vortex displaced from the center of N is equal to the derivative of $\varepsilon(c)$ (Fig. 7). The greatest force is obtained when the vortex passes the SN boundary. This is expected, since the derivative of the zero-field order parameter is greatest at the boundary. Note that curve C in Fig. 7 has a very sharp maximum at the SN interface compared to the maximum on curve A. This indicates that for small coherence length ξ_N the line energy changes rapidly when the vortex core passes the small region around the interface, with a width of the order of ξ_N and ξ_S in N and S, respectively.

Next we calculate the force acting on the vortex placed at the SN interface, for different barrier thicknesses and fixed ξ_N. The results are shown in Fig. 8. For small normalized thickness $2a_N/\xi_N$, the force for $\xi_N = 0.4$ is smaller than the force for $\xi_N = 2$. At greater $2a_N/\xi_N$ the coupling between the vortex and N is greater for smaller coherence lengths. The two curves intersect when $a_N \approx \xi_N$.

Better understanding of these results is possible if we look separately at the magnetic and the core interaction, defined as the derivative of the magnetic and the core-position-dependent energy, respectively. Let us consider first the connection between the magnetic interaction and the supercurrent distribution.

For small normalized thicknesses ($2a_N/\xi_N < 1$) supercurrents around a single vortex in the superconductor near the interface are weakly perturbed by N in both the "conventional" $\xi_N = 2$ and the "model" $\xi_N = 0.4$ cases, because the order parameter is not strongly reduced in N. For larger thicknesses the influence of the N layer on the supercurrent distribution depends on ξ_N.

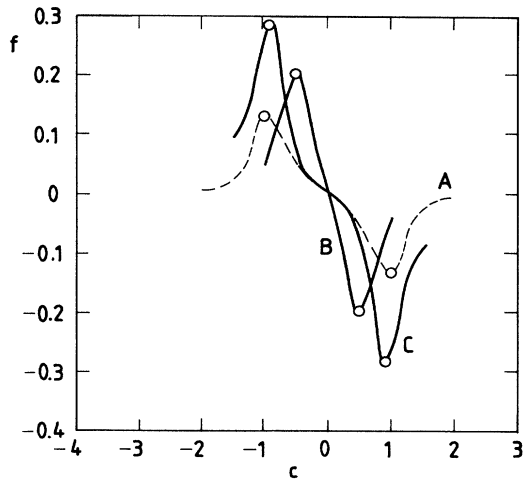

FIG. 7. Force f acting on the vortex at distance c from the center of N: A, $\xi_N = 2$, $a_N/\xi_N = 0.5$ (dashed line); B, $\xi_N = 0.4$, $a_N/\xi_N = 1$ and C, $\xi_N = 0.4$, $a_N/\xi_N = 2$ (solid lines). Each line is obtained by differentiating the position-dependent line energy in Fig. 6. The circles give the position of SN interfaces. The GL parameters are $\kappa_S = 5$ and $\kappa_N = 0.2$ for each line. All quantities are in reduced units.

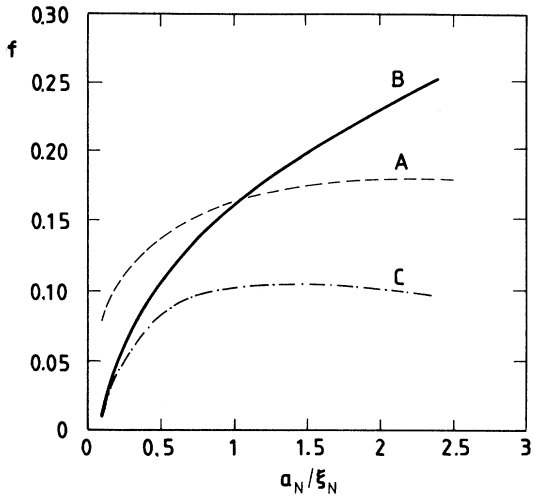

FIG. 8. Reduced force f acting on the vortex located at the SN interface vs a_N/ξ_N: A, $\xi_N = 2$; B, $\xi_N = 0.4$. The GL parameters are $\kappa_S = 5$ and $\kappa_N = 0.2$. Curve C is the core interaction vs a_N/ξ_N corresponding to curve B.

Figure 2(b) provides a plot of the supercurrent distribution around a single vortex located in the superconductor at distance $c = 0.4$ from the interface, for the N-metal thickness $2a_N = 1.6$ and $\xi_N = 0.4$. Streamlines are condensed in the region between the center of the vortex and the SN interface. This pattern resembles the set of streamlines that would result from the superposition of the supercurrents of the vortex and its image[12] on the opposite side from the SN interface. On the other hand, our results show that for $\xi_N = 2$ streamlines are not much disrupted by the N layer with the same normalized thickness, because screening in N is effective in the region near the SN interface of width $\approx \xi_N$, larger than λ_S. Thus, the increase of a_N/ξ_N causes significant increase of the magnetic interaction when the coherence length is small ($\xi_N = 0.4$). When the coherence length is large ($\xi_N = 2$), magnetic interaction saturates rapidly with increasing a_N/ξ_N.

Core interaction behaves similarly both for $\xi_N = 0.4$ and $\xi_N = 2$, saturating at $a_N \approx \xi_N$ and being as much stronger as the coherence length ξ_N is larger. Curve C in Fig. 8 shows the variation of the core interaction for $\xi_N = 0.4$ when the N-layer thickness increases. Core interaction remains practically constant when $a_N > \xi_N$.

Thus, the intersection of curves A and B in Fig. 8 comes from a rapid increase of magnetic interaction when $a_N > \xi_N$, occurring when the N-metal coherence length is small compared with λ_S ($\xi_N = 0.4$).

Therefore, the behavior of the total pinning force acting on an isolated vortex results from the addition of the magnetic and the core interaction. The magnitude of the magnetic interaction depends very much on the coherence length ξ_N. When the barrier thickness is large ($a_N > \xi_N$), it is as much stronger as ξ_N is smaller. For ξ_N greater than λ_S magnetic interaction remains smaller

than the core interaction.

We can expect that in HTC oxides, with very small coherence length ξ_N, microdefects provide strong pinning centers because they produce a significant decrease of the line energy at a distance of the order of ξ_N from the SN interfaces. Both magnetic and core pinning mechanisms pin the vortex to the defect, the magnetic interaction being larger than the core interaction in this case.

III. *SNS* JUNCTION IN HTC LIMIT

A. Approximate solution of the magnetic field equation

1. Formulation

We consider next the magnetic field and the current distribution produced by a vortex in a SNS junction in the limit

$$\kappa_S \gg 1 \ , \ \xi_N(T_c) \sim \xi_S(0) \ , \ a_N \ll \lambda_S(0) \ . \tag{18}$$

In a homogeneous high-κ_S superconductor the size of the vortex core ξ_v is considerably smaller than λ_S, and the line energy is approximately equal to the magnetic energy. The same approximation can be used for the SNS junction under the conditions of (18). Assuming that $\xi_v \sim \xi_S$, we neglect the core effects in Eqs. (10) and (11), putting $f = 1$. As before, all quantities will be expressed in reduced units, and we shall consider the case $T_{cN} = 0$. In the present case, at temperatures not too close to zero, $\kappa_{SN} \gg 1$, and the field is essentially not screened in N,[14] so that the magnetic energy is located practically outside N. To solve Eq. (11), we use the Fourier transform

$$h(x,y) = (1/2\pi) \int dq \, e^{iqy} c_q(x) \ .$$

Then, Eq. (11) becomes

$$\left(1 + \frac{q^2}{g^2}\right) c_q(x) - \frac{d}{dx}\frac{1}{g^2}\frac{dc_q(x)}{dx} = \frac{2\pi}{\kappa_S}\delta(x) \ . \tag{19}$$

Function $g(x)$ is different from 1 in a small interval that comprises the defect N and a region of order ξ_S in S on each side of the defect. We denote this region by M. The reduced thickness of M is of order $1/\kappa_S$. Outside M we get

$$(1+q^2)C_q(x) - \frac{d^2C_q(x)}{dx^2} = \frac{2\pi}{\kappa_S}\delta(x) \ , \tag{20}$$

where $C_q(x)$ denotes the approximate solution of Eq. (19), which is asymptotically equal to $c_q(x)$ outside M. We shall solve Eq. (20) in each half-space outside of M separately. In order to obtain the boundary conditions at the defect, we distinguish two cases: vortex centered in the defect, $c = 0$ and vortex outside M, $|c| \gg 1/\kappa_S$.

2. Vortex centered in the defect

In this case outside M δ function is zero. To derive the boundary conditions for Eq. (20) we integrate Eq. (19) in the interval $(-R, R)$, where $(1/\kappa_S) \ll R \ll 1$. In this interval function $c_q(x)$ is practically constant, but $g(x)$ is not, so that we get

$$\left(\frac{dc_q}{dx}\right)_{x=-R} - \left(\frac{dc_q}{dx}\right)_{x=R} = \frac{2\pi}{\kappa_S} - c_q(0)[\ 2R(1+q^2) + \Gamma q^2] \ , \tag{21}$$

where $\Gamma = \int dx \, (g^{-2} - 1)$. Explicitly,

$$\Gamma = 2\sqrt{2}\left[\coth\left(\frac{b\kappa_S}{\sqrt{2}}\right) - 1\right]\frac{1}{\kappa_S} + \xi_N \sinh\left(\frac{2a_N}{\xi_N}\right)\coth^2\left(\frac{b\kappa_S}{\sqrt{2}}\right) - 2a_N \ . \tag{22}$$

When $x \approx \pm R$, $c_q(x)$ is asymptotically equal to the solution $C_q(x)$, and $c_q(0) = C_q(0)$, with accuracy $c_q(0)/\kappa_S$ when $a_N \sim 1/\kappa_S$. Now, in the scale of λ_S, characterizing the variation of C_q, $R \ll 1$ and in this limit Eq. (21) gives the boundary condition for Eq. (20):

$$\left(\frac{dC_q}{dx}\right)_{x=-0} - \left(\frac{dC_q}{dx}\right)_{x=+0} = \frac{2\pi}{\kappa_S} - C_q(0)\Gamma q^2 \ . \tag{23}$$

The solution of Eq. (20) satisfying Eq. (23) is

$$C_q(x) = \frac{1}{1 + \Gamma q^2/2\sqrt{1+q^2}} C_q^0(x) \ , \tag{24}$$

where

$$C_q^0(x) = \frac{\pi}{\kappa_S\sqrt{1+q^2}} \exp\left(-|x|\sqrt{1+q^2}\right) \tag{25}$$

is the solution without the N layer. We also studied the numerical solution of Eq. (19), taking $g(x)$ as constant outside the defect and $a_N \sim 1/\kappa_S$. The result is that the relative difference between C_q and the numerical solution is of the order of $1/\kappa_S$.

Therefore, N changes the structure of the vortex through the term $C_q(0)\Gamma q^2$ in Eq. (23), which becomes as important as the generating term $2\pi/\kappa_S$ when Γ becomes of the order of 1. This condition is realized when the order parameter in N is strongly reduced: at any temperature T when

$$\xi_N \sinh\left(\frac{2a_N}{\xi_N}\right) \sim 1 \tag{26}$$

and at any normalized thickness $2a_N/\xi_N(T_c) > 0$ when

$$|1 - T/T_c| \sim \left(\frac{1}{\kappa_S}\sinh\frac{2a_N}{\xi_N}\right)^2 \ . \tag{27}$$

For $\xi_N \approx \xi_S$, the condition given in Eq. (26) becomes

$$a_N \sim \frac{1}{2\kappa_S}\ln(2\kappa_S) = a_N^* \ . \tag{28}$$

For example, when $\kappa_S = 100$, for $a_N/\xi_N \sim 2.6$ the solution is strongly perturbed by N. The characteristic "magnetic" thickness a_N^*, which gives the thickness of N that strongly perturbs the field of the vortex, is considerably greater than the relevant thickness, of the order of ξ_N, for the change of the core energy. When $a_N \approx \xi_N$, the core energy of the vortex is significantly reduced from its bulk value, while the magnetic energy, which is the main part of the line energy, is still approximately equal to the bulk value and becomes reduced only in a narrow temperature interval around T_c defined by Eq. (27). When the thickness of the barrier $2a_N$ becomes greater than $2a_N^*$, Eq. (27) is satisfied in the whole temperature interval, except in a narrow temperature interval near $T = 0$.

Next we calculate the line energy of the vortex, which is now

$$\varepsilon(0) = \frac{\kappa_S}{4\pi} \int \frac{dq}{2\pi} \int dx \left[\left(1 + \frac{q^2}{g^2}\right) c_q^2 + \frac{1}{g^2} \left(\frac{dc_q}{dx}\right)^2 \right] .$$

The core of the vortex is modeled by the introduction of a core-radius cutoff of order $1/\kappa_S$, as in the usual London model.[13] Then,

$$\varepsilon(0) = \frac{1}{2} \int \frac{dq}{2\pi} c_q(1/\kappa_S) \approx \frac{1}{2} \int \frac{dq}{2\pi} C_q(1/\kappa_S)$$

and

$$\varepsilon(0) = \frac{1}{\kappa_S} \int_0^\infty dq \frac{\exp\left(-\sqrt{1+q^2}/\kappa_S\right)}{2\sqrt{1+q^2} + \Gamma q^2} . \tag{29}$$

When $a_N/\xi_N \to 0$, $\varepsilon(0) \to \ln(\kappa_S)/2\kappa_S$ with a logarithmic accuracy. In the opposite limit $\Gamma \gg 1$,

$$\varepsilon(0) \approx \frac{\pi}{2\kappa_S\sqrt{2\Gamma}} . \tag{30}$$

If Γ is much greater than 1, either Eq. (26) or Eq. (27) is satisfied. In these two cases, the lower critical field in physical units is

$$H_{c1} = \frac{\Phi_0}{4\lambda_B\sqrt{\xi_N\lambda_S}} \exp\left(-\frac{a_N}{\xi_N}\right) , \; a_N \gg a_N^* , \tag{31}$$

where λ_B is the local penetration depth at the SN interface, defined below Eq. (13), and

$$H_{c1} = \sqrt{2} H_c(T) \frac{\pi}{4} \sqrt{\frac{\xi_N(T_c)/\lambda_S(0)}{\sinh(2a_N/\xi_N)}} \times \left(1 - \frac{T}{T_c}\right)^{1/4} , \; T \to T_c . \tag{32}$$

The first calculation of the lower critical field H_{c1} in a SNS junction was carried out by Dobrosavljević and de Gennes[11] (DG). It was found that

$$H_{c1} = \frac{\Phi_0}{4\lambda_B\sqrt{\xi_N(a_N - \rho)}} \exp\left(-\frac{a_N}{\xi_N}\right) , \; a_N/\xi_N \gg 1 , \tag{33}$$

where parameter $\rho = \xi_N \ln(0.89\xi_N/\lambda_B)$. Equations (31) and (33) give very similar expressions for H_{c1}, the only difference arising between lengths λ_S and $a_N - \rho$. The result of DG is valid when the vortex is wholly contained in the N layer, and it is obtained by variational method assuming a reasonable analytic form for the magnetic field of the vortex, i.e., that the field in N is constant along x up to a distance ρ of the SN interfaces and is zero beyond that. This assumption is valid for thick N layer, in the limit $\kappa_{SN} \ll 1$,[14] where κ_{SN} is defined by Eq. (13). However, in the limit given by Eq. (18), $\kappa_{SN} \gg 1$, and a reasonable functional form for the magnetic field is $h(x) = h(0)\exp(-|x|/\lambda_S)$. Then, the variational principle gives exactly Eq. (31).

3. *Vortex deep in the superconductor*

Now, in the region outside M, the δ function in Eq. (20) is different from zero. Integrating Eq. (19) in the interval $c - R < x < c + R$, and making the same assumptions as in the previous case, we get the following boundary condition:

$$\left(\frac{dC_q}{dx}\right)_{x=c+0} - \left(\frac{dC_q}{dx}\right)_{x=c-0} = C_q(c)\Gamma q^2 . \tag{34}$$

The corresponding boundary condition for the magnetic field is

$$\left(\frac{\partial h}{\partial x}\right)_{x=c+0} - \left(\frac{\partial h}{\partial x}\right)_{x=c-0} = -\Gamma \left(\frac{\partial^2 h}{\partial y^2}\right)_{x=c} .$$

Therefore, the supercurrent in the direction parallel to the layer has the y-dependent jump, when either Eq. (26) or (27) is satisfied. The solution of Eq. (20) satisfying this boundary condition is

$$C_q(x) = C_q^0(x) - \frac{C_q^0(c)\, C_q^0(x-c)}{C_q^0(0)} \frac{1}{1 + 2\sqrt{1+q^2}/(\Gamma q^2)} . \tag{35}$$

Again, numerical studies of Eq. (19) showed that the accuracy of this solution is $1/\kappa_S$. $C_q^0(x)$ is the solution without the N layer and the term $-C_q^0(c)C_q^0(x-c)/C_q^0(0)$ is a Fourier-transformed field produced by the image of the vortex,[12] on the other side of N. The image of the vortex is screened, with the q-dependent screening constant

$$\epsilon(q) = 1 + 2\sqrt{1+q^2}/\Gamma q^2 .$$

In the limits $T \to T_c$ or $a_N \gg a_N^*$, $\epsilon(q) \to 1$, and therefore the image is not screened. If $a_N/\xi_N \to 0$, then $\epsilon(q) \to \infty$, the image is completely screened, and the homogeneous solution $C_q^0(x)$ is recovered. The dependence of the screening constant upon the wavelength $2\pi/q$ means that the image is spread out in the direction parallel to N at distance c from the N layer on the opposite side from the original vortex.

Next we evaluate the line energy, which now consists of "bare" energy $\varepsilon_0 \approx \ln(\kappa_S)/2\kappa_S$ and the interaction

energy with the image $U(c)$: $\varepsilon(c) = \varepsilon_0 - U(c)$,

$$U(c) = \frac{1}{2\kappa_S}\int_0^\infty dq\,\frac{1}{\epsilon(q)}\frac{\exp\left(-2|c|\sqrt{1+q^2}\right)}{\sqrt{1+q^2}} . \tag{36}$$

For $c \gg 1$, the image term $U(c)$ vanishes as e^{-2c}. At $c \sim 1/\kappa_S$, $U(c)$ must be altered so that $\varepsilon(c)$ goes smoothly to the value given by Eq. (29), rather than going to $-\infty$ with $\ln(2|c|)$.

The derivative of the line energy $d\varepsilon/dc$ gives the attractive magnetic force:

$$f(c) = \frac{1}{\kappa_S}\int_0^\infty dq\,\frac{\exp\left(-2|c|\sqrt{1+q^2}\right)}{1+2\sqrt{1+q^2}/(\Gamma q^2)} . \tag{37}$$

The greatest value of the force is obtained for the lowest allowed value of c, which is of order $1/\kappa_S$. We choose this limiting value c^* so that $\varepsilon(c)$ is smooth and goes linearly to $\varepsilon(0)$ when $c < c^*$:

$$\varepsilon(0) + f(c^*)c^* = \varepsilon(c^*) ,$$

i.e., we assume that the magnetic energy has a kink at the point $c = c^*$. The variation of $f(c^*)$ when a_N/ξ_N increases is shown in Fig. 9. We note that f saturates when Eq. (26) is satisfied rather than at $a_N/\xi_N \sim 1$ when the core interaction saturates. This behavior is expected, because numerical results in Sec. II indicated that the magnetic force continues to increase even though the core interaction is saturated.

The limiting value c^* depends weakly on the material parameters, and, typically, it is in the interval $(1/\kappa_S, 1.3/\kappa_S)$. For such small c^*, magnetic interaction is approximately equal to

$$f(c) \approx \frac{1}{2\kappa_S c}\left[1 - \frac{4c}{\Gamma}\exp\left(\frac{4c}{\Gamma}\right)E_1\left(\frac{4c}{\Gamma}\right)\right] ,$$

where $E_1(x) = \int_x^\infty dt\, e^{-t}/t$.

For a vortex located deep in the superconductor, total force between the vortex and the N phase is equal to the attractive magnetic interaction given by Eq. (37). When c becomes of the order of $1/\kappa_S$, the vortex core passes through the region M, and the core interaction has to be considered in addition to the magnetic interaction. It is equal to the derivative of the core energy in Eq. (12), and it is greatest at the SN interface. For simplicity, we assume $\kappa_N = 0$ and $\xi_v = \sqrt{2}/\kappa_S$.[17] Then, curve f_c in Fig. 9 shows that the core interaction saturates at $a_N \approx \xi_N$ and that it is approximately one-fourth of $f(c^*)$ when the total force saturates.

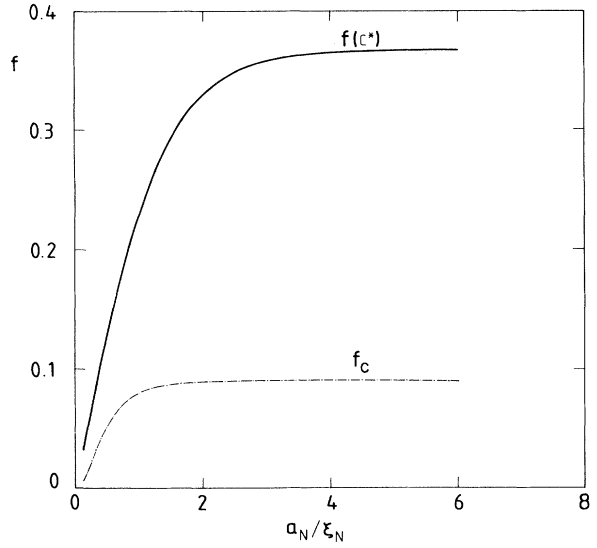

FIG. 9. Reduced force f acting on a vortex displaced from the N layer vs a_N/ξ_N: magnetic force $f(c^*)$ is defined by Eq. (37) and the core interaction force f_c equal to the derivative of the position-dependent core energy at the SN interface, for $\xi_v = \sqrt{2}/\kappa_S$. The GL parameters are $\kappa_S = 100$ and $\kappa_N = 0$, and the coherence length of the N layer is $\xi_N = \lambda_S/\kappa_S$.

B. Temperature dependences of H_{c1} and J_c

Now, it is easy to extract the temperature dependence of the lower critical field $H_{c1}(T)$ and the critical current density $J_c(T)$ from the previous results.

The temperature dependence of the coherence length in the N phase is

$$\xi_N^2(T) = \hbar^2/2m\alpha_N(T) = \xi_N^2(T_c)T_c/T ,$$

where it is assumed that $T_{cN} = 0$. In reduced units we get

$$\xi_N(t) = \xi_N(1)\sqrt{(1-t)/t} \tag{38}$$

and $a_N(T) = a_N(0)\sqrt{1-t}$, since $\lambda_S(t) = \lambda_S(0)/\sqrt{1-t}$, where $t = T/T_c$, $\xi_N(1) = \xi_N(T_c)/\lambda_S(0)$, and $a_N(0) = a_N/\lambda_S(0)$. Then, $H_{c1}(T) = \sqrt{2}H_c(T)\varepsilon(0)$.

In the limit $T \to T_c$, when Eq. (27) is satisfied, H_{c1} vanishes as $(1-t)^{1.25}$. This rather unusual behavior originates from a well-known characteristic of a proximity system: The order parameter at the SN interface vanishes as $(1-t)$ rather than as $\sqrt{1-t}$ in bulk superconductor [see Eqs. (7) and (8)]. Taking parabolic temperature dependence for the thermodynamic critical field $H_c(T) = H_c(0)(1-t^2)$, rather than the GL dependence $H_c(T) \propto (1-t)$, valid near T_c, we plot $H_{c1}(T)$ in Fig. 10. Various curvatures are obtained for different $a_N/\xi_N(T_c)$. When $a_N/\xi_N(T_c) = 1$, the curvature is negative in the whole temperature interval except in the extremely narrow region near T_c. This negative curvature originates from the negative curvature of $H_{c1}(T)$ in the bulk superconductor. When $a_N/\xi_N(T_c) = 3$, the thickness of N is greater than the magnetic thickness $2a_N^*$, and Eq. (27) is satisfied in the whole temperature interval. As a result, negative curvature in H_{c1} for bulk superconductor is completely suppressed. This suppression becomes extreme when $a_N/\xi_N(T_c) \sim 7$: $H_{c1}(T)$ reveals a drastic increase when t decreases at low temperatures.

The explanation of various curvatures observed in

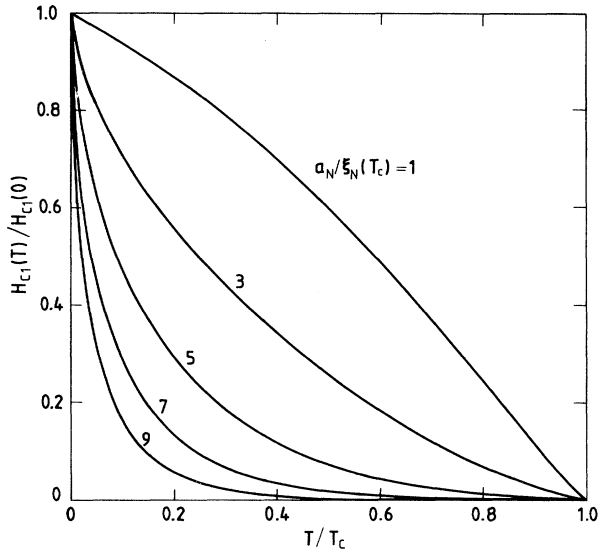

FIG. 10. Temperature dependence of the lower critical field H_{c1} of the SNS junction with the GL parameters $\kappa_S = 100$ and $\kappa_N = 0$, and the coherence length of the N layer at the critical temperature T_c of the superconductor $\xi_N(T_c) = \lambda_S(0)/\kappa_S$, for different barrier thicknesses $2a_N$.

HTC oxides becomes very simple. The anisotropy of the crystal does not qualitatively change the obtained temperature dependence, since anomalous $H_{c1}(T)$ dependence originates from the strong reduction of the zero-field order parameter in the defect. As before, suppose that the defect is perpendicular to the c axis and that the field is parallel to the defect. Then, the coherence lengths ξ_S and ξ_N characterize the order parameter's spatial variation along the c direction, and the above-described temperature dependence applies to the field $H_{c1}^{\perp}$ perpendicular to the c axis. $H_{c1}^{\perp}$ exhibits anomalous temperature dependence when the thickness of the defect is of order or greater than the magnetic thickness $2a_N^*$. For example, if $\kappa_S = 300$ the defect causing anomalous behavior is thicker than $5\xi_S(0)$, where it is assumed that $\xi_S(0) \approx \xi_N(T_c)$. Therefore, the proximity-induced anomalous $H_{c1}^{\perp}(T)$ dependence originates from the N phase extending over the region of several unit cells, and it is not an intrinsic property of the superconducting phase. On the other hand, weak logarithmic dependence of a_N^* upon κ_S gives thicknesses of N phases much smaller than λ_S. Therefore, these defects may exist even in very small single crystals. Negative curvature in $H_{c1}^{\perp}(T)$, observed in Refs. 1 and 2, still allows presence of N phases of thicknesses less than the magnetic thickness, so that the influence of N on H_{c1} is small.

Next, we find the temperature dependence of the critical current density $J_c(T)$ for the displacement of a single vortex from the N defect. If the largest pinning force per unit vortex length is F (in physical units), then the critical current is determined from the balance between the Lorentz force $\Phi_0 J_c/c$ and F: $J_c = cF/\Phi_0$, or

$$J_c = \frac{c\Phi_0\kappa_S}{8\pi^2\lambda_S^3} f \ ,$$

where f is the derivative of the line energy ε, given by Eq. (12), at the SN interface.[18] The magnetic energy $\varepsilon_m = h(0,0)/2$ gives the magnetic interaction

$$f_m = \left(\frac{d\varepsilon_m}{dc}\right)_{c=a_N} = \left[\left(\frac{\partial\varepsilon_m}{\partial c}\right)_{\xi_v} + \left(\frac{\partial\varepsilon_m}{\partial\xi_v}\right)_c \frac{d\xi_v}{dc}\right]_{c=a_N} .$$

The remaining part of the line energy ε_c gives the core interaction:

$$f_c = \left(\frac{d\varepsilon_c}{dc}\right)_{c=a_N} = \left[\left(\frac{\partial\varepsilon_c}{\partial c}\right)_{\xi_v} + \left(\frac{\partial\varepsilon_c}{\partial\xi_v}\right)_c \frac{d\xi_v}{dc}\right]_{c=a_N} .$$

Since parameter ξ_v is obtained from $[\partial(\varepsilon_m + \varepsilon_c)/\partial\xi_v]_c = 0$, we get

$$f_m = \left[\left(\frac{\partial\varepsilon_m}{\partial c}\right)_{\xi_v} - \left(\frac{\partial\varepsilon_c}{\partial\xi_v}\right)_c \frac{d\xi_v}{dc}\right]_{c=a_N} ,$$

so that in total force the contributions $\propto d\xi_v/dc$ cancel, and $f = f_m + f_c$ can be approximated by

$$f \approx f(c^*) + \left(\frac{\partial\varepsilon}{\partial c}\right)_{\sqrt{2}\xi_S} . \tag{39}$$

The approximation $\xi_v \approx \sqrt{2}\xi_S$ used in f_c does not qualitatively change the results. The resulting critical current densities $J_c = J_c^m + J_c^c$, with J_c^m and J_c^c corresponding to $f(c^*)$ and $(\partial\varepsilon_c/\partial c)_{\sqrt{2}\xi_S}$, respectively, are shown in Figs. 11 and 12. J_c has maximum at the temperature, which is as much lower as the thickness of N is larger. Since $f(c^*)$ vanishes at zero temperature, $J_c \to J_c^c$ when $t \to 0$.

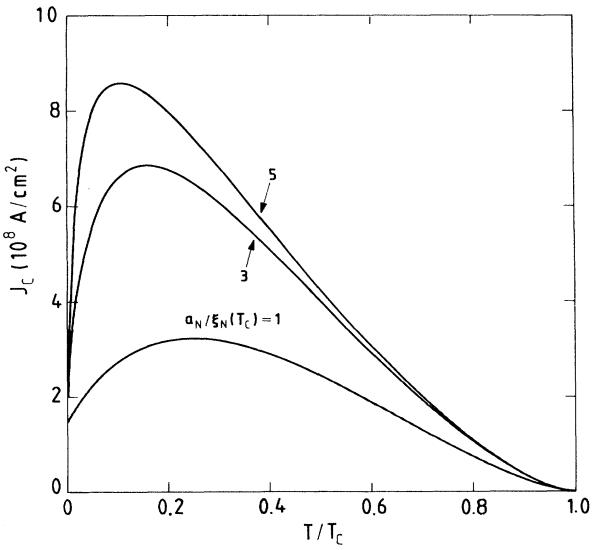

FIG. 11. Temperature dependence of the critical current density J_c for the displacement of an isolated vortex from the SNS-modeled microdefect, with $\kappa_S = 100$ and $\kappa_N = 0$, $\lambda_S = 10^3$ Å, and the coherence length $\xi_N(T_c) = \lambda_S(0)/\kappa_S$, for $a_N/\xi_N(T_c) = 1$, 3, and 5.

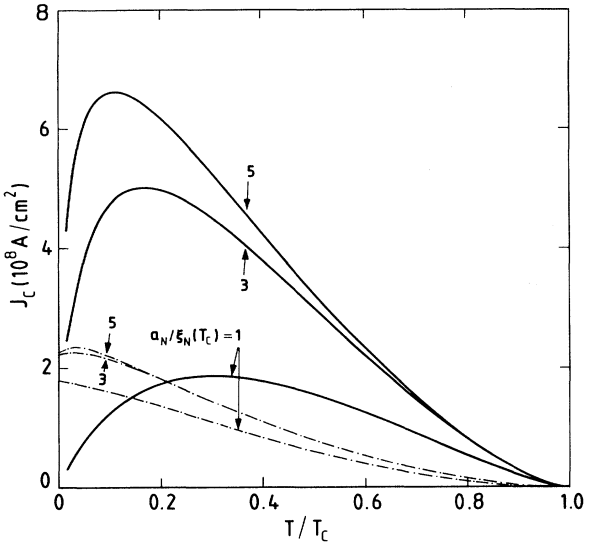

FIG. 12. Temperature dependence of parts J_c^m and J_c^c of the critical current density for the displacement of an isolated vortex from the SNS-modeled microdefect, with $\kappa_S = 100$ and $\kappa_N = 0$, $\lambda_S = 10^3$ Å, and the coherence length $\xi_N(T_c) = \lambda_S(0)/\kappa_S$, for $a_N/\xi_N(T_c) = 1$, 3, and 5. J_c^m: solid lines; J_c^c: dot-dashed lines.

For $a_N/\xi_N(T_c) = 1$, Eq. (27) is not satisfied (except very close to T_c) and the critical current has no pronounced maximum as a function of T.

If $a_N/\xi_N(T_c) \sim 3$, the thickness of the defect is comparable to the magnetic thickness. In this case, Eq. (27) is satisfied even at low T, and J_c increases rapidly with temperature, due to the rapid increase of $f(c^*)$. This increase corresponds to the drastic increase in anomalous $H_{c1}(T)$ dependence at low temperatures. At higher temperatures, the term $f(c^*)$ in Eq. (39) dominates, and, therefore, the interaction between a vortex and this defect is primarily magnetic (see Fig. 12). After the maximum J_c slowly decreases.

This behavior of thick defects ($a_N \sim a_N^*$) results from the change of the supercurrent distribution around the vortex in the superconductors with temperature. Recall that the screening of the vortex field in the defect is effective only in the region of thickness $\sim \xi_N$ near the interfaces (screening region). At low T, so that $\xi_N \gg a_N$, the supercurrent distribution is almost unperturbed. With increasing T, ξ_N rapidly decreases, becoming smaller than the thickness of the defect. Then, the supercurrent density decays exponentially in the defect and the screening region is located near the interfaces. Since this region is much smaller than λ_S, the streamlines, in the scale of λ_S, seem squeezed to the interface. Thus, the supercurrent distribution is strongly perturbed at higher temperatures. Then, if the vortex moves from S to N, the supercurrent distribution changes drastically when the vortex core passes the screening region of the defect. In this region, the vortex transforms into the weak vortex[19] having energy $\varepsilon(0)$ in the center of N.[20] This change causes a strong magnetic interaction at higher T.

For typical values of parameters $\xi_S(0) \sim 10$ Å, $\kappa_S \sim 100$, and $\lambda_S \sim 2000$ Å our model gives that J_c is of the order of magnitude 10^7–10^8 A/cm^2. We conclude that the pinning of vortices on N phases in HTC oxides causes very large critical currents in single crystals.[21] In order to check the predicted behavior experimentally, the easiest way would be to measure the temperature dependence of J_c in a HTC S/N superlattice, with the current and the external magnetic field $H^{\text{ext}} \gtrsim H_{c1}(T)$ in the plane of the layers, and with the appropriate choice of S and N thicknesses a_S and a_N ($a_S \sim \lambda_S$, $a_N \sim \xi_N \ln \kappa_S$).

IV. CONCLUSION

In this paper we have shown how a single defect, modeled by a SNS junction, can lead to different curvatures in $H_{c1}(T)$ dependence. In HTC superconducting single crystals a set of separated microdefects, each modeled by an N layer, would lead to similar $H_{c1}(T)$ dependence (although the Meissner state would be gradually destroyed by the successive field penetration through various N "channels"). Assuming that the characteristic coherence lengths for the superconducting and for the normal phase are similar, we find that the thickness of the defects producing anomalous $H_{c1}(T)$ dependence is of the order of or greater than the magnetic thickness $2a_N = \xi_S \ln \kappa_S$. This leads to the defects that are significantly larger than the crystal unit cell.

Our study of the interaction between a vortex and the N defect shows that this interaction produces strong critical currents for the displacement of an isolated vortex. This interaction is primarily magnetic at high temperatures, due to the formation of narrow screening regions in the defect, which are located only near the interfaces. At low temperatures (when the coherence length in the defect is large) magnetic interaction is reduced.

ACKNOWLEDGMENTS

We would like to thank Marko Ledvij and Zoran Radović for helpful discussions and useful suggestions. This work is supported in part by Grant No. JF 898 under the National Science Foundation's U.S.-Yugoslavia Cooperative Research Program.

[1] L. Krusin-Elbaum, A. B. Malozemoff, Y. Yeshurun, D. C. Cronemeyer, and F. Holtzberg, Phys. Rev. B **39**, 2936 (1988).
[2] S. Sridhar, Dong-Ho Wu, and W. Kennedy, Phys. Rev. Lett. **63**, 1873 (1989).
[3] T. Ishii and T. Yamada, Physica C **159**, 483 (1989).
[4] H. Adrian, W. Assmus, A. Höhr, J. Kowalevski, H. Spille, and F. Steglich, Physica C **162–164**, 329 (1989).

[5]D. Hirashima and T. Matsuura, J. Phys. Soc. Jpn. **59**, 24 (1990).
[6]Z. Ye, H. Umezawa, and R. Teshima (unpublished).
[7]T. Koyama, N. Takezawa, and M. Tachiki, Physica C **168**, 69 (1990).
[8]R. Baskaran, Y. Hariharan, M. P. Janawadakar, and T. S. Radhakrishnan, Physica C **158**, 406 (1989).
[9]A. G. Khachaturyan and J. W. Morris, Jr., Phys. Rev. Lett. **59**, 2776 (1987).
[10]D. J. Werder, C. H. Chen, R. J. Cava, and B. Batlogg, Phys. Rev. B **38**, 5130 (1988).
[11]L. Dobrosavljević and P. G. de Gennes, Solid State Commun. **5**, 177 (1967).
[12]C. P. Bean and J. D. Livingston, Phys. Rev. Lett. **12**, 14 (1964).
[13]M. Tinkham, *Introduction to Superconductivity* (McGraw-Hill, New York, 1975).
[14]Orsay Group on Superconductivity, in *Quantum Fluids*, edited by D. F. Brewer (North-Holland, Amsterdam, 1966), p. 26.
[15]D. F. Cowen, M. I. Hartzell, M. P. Zaitlin, and W. E. Lawrence, Phys. Rev. B **30**, 1194 (1984).
[16]P. G. de Gennes, *Superconductivity of Metals and Alloys* (Benjamin, New York, 1966).
[17]J. R. Clem, J. Low Temp. Phys. **18**, 427 (1975).
[18]Note that our reduced units for the energy and force differ by a factor of $\kappa_S/(4\pi)$ from the standard ones; see the text below Eq. (11).
[19]Yu. P. Denisov, Fiz. Tverd. Tela (Leningrad) **18**, 119 (1976).
[20]Note that the length scale for the variation of the line energy changes when the vortex core passes the interface. This scale is λ_S for the vortex deep in the superconductor, and it becomes ξ_N ($\sim \xi_S$) for the vortex passing through the defect. In the HTC limit, this change appears as a divergence in $f(c)$ at $c = 0$.
[21]M. Tachiki and S. Takahashi, Solid State Commun. **70**, 291 (1989).